Discover of No-Side Effect Phenytoin Drug from Catharanthus Roseus Plant

Nagaraj Govindan (thomsun1977@gmail.com)
Periyar University PG Extension Center

Article

Keywords: Catharanthus Roseus, Phenytoin drug, no side effect, drug development, nano-sized plant

Posted Date: March 3rd, 2021

DOI: https://doi.org/10.21203/rs.3.rs-273643/v1

Abstract

Phenytoin drug is commonly used for seizures and breast cancer, but chemically prepared phenytoin drug has more side effect. Herein, we have discovered phenytoin drug (100%) without side effect from Catharanthus Roseus (CR) plant using a photon-induced method (PIM). The pure plant (absence of metal nanoparticles) synthesized by green chemistry offers a novel and potential alternative to non-chemically synthesized Catharanthus Roseus nano-sized particles (CR-NPs,) studied for the first time. The GC-MS analysis of CR-NPs provides all peaks determining the presence of phenytoin compound and 1H NMR analysis of chemical shift conformed phenytoin structure. The XRD analysis results in highly crystalline material and crystallite size is 25 nm. The CR NPs highly killed breast cancer cells (MCF-7 cell-lines), while without killed the normal cells (VERO cell-lines). Our findings brought new insights into the development of nano-sized plant exerting strong next generation of no-side effect nature drug.

Background

Nano-scale research, the use of innovative medicinal prepared at nano-scale levels is widespread worldwide. The researchers make an effort to discover an eco-friendly process for the fabrication of green nanoparticles (NPs).[1] The green synthesis has great attention to synthesizing metal NPs from medicinal plants and these NPs has been multifunctional and has an interesting application in agricultural, medical, and physical fields [2]. Currently, NPs are crucial in producing sustainable technologies for modern society. Nanotechnology has several drawbacks such as high-cost processing, difficult to manufacture and incorporates nano-pollution, which is extremely dangerous for living organisms.[3,4] Developing NPs for drug delivering system is extensive due to the use of chemicals as a detergent that impacts on climate. In addition, drug delivery with NPs demonstrates toxicity, predictable gelation tendency, alveolar inflammation, and burst release.[5,6] The literature studies on the biosynthesized of metal NPs from an extract of the plant are common. But, the current work reports on employing a novel PIM technique for tapping the rich reservoirs of bioactive materials as CR NPs from CR plants. PIM created the nano-packets of active metabolites that revealed improved solubility in solvents and enhanced biologically active pharmaceutical properties. Nowadays, NPs synthesized from medical plants, as therapeutic agents gain much more attention compared to conventional therapy nano-medicine, have side effects on human healthcare. Moreover, eco-friendly biosynthesized of plant NPs is may have a huge impact on the control of various chronic diseases.[7,8]

GC-MS technique can be employed for the study the bio-synthesized NPs and measuring the amount of some active principles in plants utilized in drugs, pharmaceutical, food or cosmetic industry.[9–12] The reported literatures on the extract materials in the investigation has demonstrated that so far there are no published papers worldwide, related to the possible nature components of biosynthesized plant NPs. Herein, we report the discovery of Phenytoin component that directly sense CR plant. In this study, attempted to synthesize green NPs (without metal trapping) evaluate as a potential breast cancer cell lines. The pure biological synthesis of plant NPs may be most effective and provide an option to

decrease the cytotoxicity, price and side effects. The production of Phenytoin from CR plants could be considered infers to the fabrication of new life-saving drugs and may have elucidated as a better alternative relative to the plant-mediated metal NPs and allopathic medicine.

Results And Discussion

To explore the crystallinity of the synthesized CR-NPs, XRD technique was conducted in the range of 05–80°. **Figure 1 (a)** displays the XRD spectrum of green synthesis CR NPs. The peaks of CR NPs were formed, the pattern showed the seven different peaks at 17.60^o, 20.02^o, 28.55^o, 40.78^o, 50.43^o, 66.69^o and 73.93^o with corresponding lattice plane value recorded at (001), (100), (101), (111), (112), (300) and (104), respectively. The above lattice plane value confirmed highly crystallite to smaller nanoparticles are formed in the case of CR-NPs are correlated to DLS and TEM measurements. The unassigned peaks, which may have occurred may be attributed to the crystalline and amorphous organic agents. The average crystalline size was evaluated from the XRD data employing the Debye-Scherrer formula. The size was found to be 25 nm in the case of CR-NPs.[13] The novel fabrication of CR-NPs compared with standard JCPDS file is not available before. The FTIR pattern of the leaf plant of CR-NPs is revealed in **Figure 1b**. The absorption bands at 3420 cm^{-1} correspond to the O-H stretching vibration. The peaks at 2922 and 2842 cm^{-1} are related with symmetric stretching and anti-symmetric of CH_2, respectively. The peak for the carbonyl groups was located at 1630 cm^{-1} due to asymmetrical COO^- stretch.[14] The carbonyl group from the amino acid and protein had a stronger capability to bind in nano-size plant particles. The low absorption peak at 1058 cm^{-1} is associated to C–O aromatic and aliphatic amines.[15] The intensive absorption peaks at 606 cm^{-1} correspond to the CR-NPs.[16]

Figure 1c and **d** show the UV-visible diffusion reflectance data modified Tauc plot. The optical direct and indirect bandgap energy (Eg) estimated from Tauc's plot was found to be 3.5 eV (**Figure1c**) and 3.09 eV (**Figure1d**).[17] These remarkably good performances can be attributed to the indirect bandgap pure plant for visible-light absorption efficiency. These data reveal that the CR-NPs can be explained by the reduced crystallinity, as shown in XRD analysis. The grain size and zeta potential was analysed by dynamic light scattering (DLS). The grain size of the green prepared CR was 19 nm with a 0.209 of PDI value. The single peak implied that the high-quality of the prepared CR plant for nano-sized particles, as shown in **Figure 2(a)**. The peak was obtained with a wide base of CR-NPs were found in the solution. The zeta potential of the CR-NPs was −0.3 mV as shown in **Figure 2(b)**, this results signifying the presence of repulsion among the synthesized nano-sized plant particles.[18] It is obvious that the CR-NPs are poly-dispersed in nature owing to its negative zeta potential and is also has long-term stability in the solution.[19] The results of FTIR was indorse the stability of CR-NPs, where it exposed two distinct peaks at 3420 and 1630 cm^{-1}.

TEM images of lower and higher magnification showed spherical shapes. The CR-NPs (**Figure 3a, b, c**) showed an average particle size varying from 10 nm to 20 nm. The nano-size particles strength avoids the passing of dissimilar molecules of protein created during the method of biosynthesis. The nano-size

particles having variable sizes and shapes was observed in common the biological organizations.[20] The TEM morphology showed in clear lattice fringes can be labelled for nanoparticles and attributed to the presence of well-crystalline NPs, as shown in **Figure 3(d)**. EDS measurements were performed, as shown in **Figure 4**. The weight percent of C (53%), O (37%) and K (10%) were obtained for CR-NPs. These results indicate that CR-NPs have more % of carbon and oxide elementals presented.[1] HNMR analysis reveals a chemical shift of CR-NPs, as shown in **Figure 5(a)**. The exhibiting different peaks, two of which assigned to the $CDCL_3$ utilized as a solvent. The main peak at 7.19 ppm corresponds to the protons of the aromatic rings. In the meantime, all the 10 protons in the structure are magnetically equivalent due to molecular equilibrium, only a single integrated signal is detected. Also, the existence of the signals only of the aromatic protons implies that phenytoin is the only compound.[21]

GC-MS analysis was used to study the chemical constituents of the CR-NPs. The test revealed that the presence of 100% phenytoin compound, as shown in **Figure 5(b)**. The GC-MS test demonstrated the presence of 2 compounds from the nano-size plant extract of CR active principles with their retention time (RT), molecular formula, peak area % and compound name are shown in **Table 1**. The compounds are identified by the mass spectroscopy were presented. The total numbers of compounds identified in the nano-sized CR plant was found as the both major and minor peak such as phenytoin compound. While micro-size particles of CR plant above 40 compounds presented was reported earlier.[22, 23] The nano-size plant of CR leaves, GC-MS results to conformed Phenytoin compound well match with CAS-57-41-0. The phenytoin compound highly bioactive of seizures, breast cancer, and diabetes.

Table 1 Chemical constituents present in the CR NPs

Peak	R. Time	Area%	Norm %	M. formula	Name
1	23.947	3.17	3.38	$C_{15}H_{12}O_2N_2$	PHENYTOIN
2	25.122	96.83	100	$C_{15}H_{12}O_2N_2$	PHENYTOIN

In-Vitro Cell Lines with No-side effect of CR-NPs

The in vitro cytotoxicity assay was conducted on normal cell lines (VERO), as shown in **Figure 6**. The control sample shown in **Figure 6(a)** and CR-NPs are non-toxic and reverts the non-toxic effect in normal cell lines as, shown in **Figure 6(b)**. The viability (%) of the NPs was illustrated through MTT assay within the VERO cell line, which showed that the CR-NPs understudy has good cell viability at all the tested concentrations (**Table 2**). The biological role of metal nanoparticles in identification and bioremediation of human cancers gained a good interest today, but all methods were both cancer and normal cells were killed. However, the pure plant of Catharanthus Roseus has attained a good name within the field of medication because of their distinctive properties that obvious therapeutic potential within the identification and treatment potential within some human cancer sorts. But, CR plant for micro-sized

particles takes treatment was a protracted time and toxic. Herein, CR micro-size converted into nano-sized CR plant for no-side effect, which confirmed in above results for the first time.

In-Vitro Cell Lines Cytotoxicity of CR-NPs

The control sample (MCF-7) is shown in **Figure 7(a)**. Toxicity rate against MCF-7 cell lines will increase with the increase within the concentration of CR-NPs, as shown in **Figure 7(b)**. The repressing impact was ascertained once 48 h of incubation. The results were exhibited as growth repressing concentration (IC_{50}) values, which represent the concentrations of the compounds needed to provide a 50% inhibition of cell growth once 48 h incubation, compared to untreated controls. The IC_{50} of cell inhibition of CR-NPs was ascertained at 15.91 µg/mL of nano-sized particles against the MCF-7 cell lines. This on top of results MCF-7 activity than others reported earlier.[24-27] The CR-NPs with different concentrations was performed on MCF-7 cell and presented in **Table 2** and **Figure 8.** CR-NPs with different concentrations on (a) Vero % cell growth and (b) MCF-7 % cell inhibition was analysed.

Table 2 VERO % cell growth and MCF-7 % cell inhibition

Concentration	VERO	MCF-7	VERO % Cell growth	MCF-7 %Cell inhibition
0	0.398	0.525		
25 µg	0.394	0.252	99.33	52.01
50 µg	0.389	0.196	97.65	62.66
100 µg	0.385	0.134	96.65	74.47

Conclusion

In summary, we discovered plant nano-sized particles via facile synthesis method (PIM) for highly effective no-side effect bioactive application. A novel technological achievement for the preparation of nano-sized plant powder was described and reported for the first time. The XRD, DLS and TEM results confirmed nano-size particles and highly crystalline particles. ^{1}H NMR and GC-MS results was structurally conserved elements along with select sequence constraints within the phenytoin compound. Oxygen binding is accompanied by conformational re-modelling of the CR-NPs, which alters the accessibility of specific regions of the phenytoin properties. The procedure is general and very advantageous to prepare micro-scale into nano-scale in good to excellent yields. The discovery of nano-sized plant powder opens new avenues for exploration. In particular, the methodology was successfully applied to the preparation of the antiepileptic drug phenytoin in good yield (GC-MS results), as the only cheap alternative to planting synthesis under photon-induced method. Our strategy can open a new frontier for safe, no-side effect, free of the cost and eco-friendly synthesis of the pharmaceutically interesting drug on nano-sized plant powder. The CR-NPs exhibited cytotoxic effects on MCF-7 cells at an IC_{50} of 15.91 µg mL^{-1} after 48 h and no-side effects were observed on normal cells line (VERO). That may well this plant proving to vast valuable no-side effect bioactive compounds are possess medicinal value than allopathic drug or plant

extract with metal nanoparticles drug. The concept of ultra-small NPs should be useful for next generation no-side effect nature drug. The green synthesis of nano-sized plant characterization may be introduced a promising applications in cosmetic, pharmaceutical industries and medicine.

Experimental Part

Materials. Catharanthus Roseus plants were provided from Dharmapuri District. The plants were cleaned with H_2O to eliminate dust and unwanted materials and it was grinned with filtered.

Nano-size plant powder preparation. The green synthesis of the plant under the photo-induced method was used for the solvent extraction procedure. About 200 ml of plant dispersion was added in 1000 ml of deionized water for 25 days under light irradiation. The resulted product was dried and annealed at 110 °C for 60 min. Characterizations Techniques: XRD patterns of the samples were monitored on a Bruker D8 Advance powder X-ray diffractometer with Cu-Kα (λ = 1.5406 Å). Elemental compositions were measured by EDX analysis (Hitachi S-4800). The morphology of NPs was ascertained via TEM (JEM-2100F). Fourier transforms infrared (FTIR) spectra of the NPs were recorded using the KBr pellet technique (Bruker, Tensor 27 spectrometer). Particle size and Z-average of samples were characterized using DLS analysis (Horiba). UV-vis Diffuse reflectance spectroscopy (UV-DRS) was obtained with a Perkin Elmer Lambda 25 spectrometer.

GC/MS analysis. GC/MS (Clarus 680 GC) was used to elucidate the existence of active constituents and the chemical composition of CR-NPs. GC/MS was accomplished employing a fused silica column consists of Elite-5MS with 95% dimethylpolysiloxane, 5% biphenyl, and 30 m × 0.25 mm ID × 250µm df. The Helium was used as carrier gas to separate the components with 1 ml/min flow. The operation temperature was maintained at 260 °C during the chromatographic process. The plant material (1µL) was applied into the device and the temperature rate was set at: 60 °C (120 s); 300 °C at the rate of 10 °C min^{-1}; and 300 °C. The mass detector was operated at: 230 °C transfer line temperature; 230 °C ion source temperature; and ionization mode electron impact at 70 eV, a scan time of 0.2 s and scan interval of 0.1 s. The spectrum of the component was compared with the data of the of known component kept in the GC-MS NIST (2008) library.

In vitro cytotoxicity of the CR-NPs Procedure. The MCF 7 cancerous and VERO normal cells were provided from National Centre for Cells Sciences. The cells were supplemented 10% fetal bovine serum (FBS) in Eagle's MEM. The samples were attained at 37ºC with 5% carbon dioxide and 95% air conditions. The culture medium was checked and maintained frequently as well as replaced twice a week.

Cells treatment protocol. The cultured cells were separated with trypsin ethylene diamine tetra acetic-acid, then viable cells were measured employing a diluted hemo-cytometer possess 5% FBS ($1x10^5$ cells/ml). Afterward, a 0.1 ml of cells solutions were added into 96-well plate at a density of 10,000 cells/well. The cells were incubated at 37 ºC with 5% carbon dioxide and 95% air. After one day of incubation, the suspensions were modified with serial contents of the prepared NPs. The samples were dispersed in

dimethylsulfoxide and sample dispersion was diluted twice and the required final test amount with serum free medium. Another four serial dilutions were performed to provide a total of five sample concentrations. A solutions of 0.1 ml of the diluted samples were inserted to the suitable wells, which having 0.1 ml of cultured media. The plates were maintained for two days at 37 ºC with similar conditions. The medium-only sample was acted as reference and triplicate was attained for all contents.

MTT assay. The mitochondrial enzymes in organ cell called succinatedehydrogenase cleave the tetrazolium and dissolving the MTT to an insoluble purple formazan. Thus, the produced formazan is precisely proportional to the viable cells number. After 2 days, 15 µl of MTT (5 mg/ml) in phosphate buffered saline was seeded to each well and kept at 37 ºC for 4 h. Then, the media with MTT were flicked off and the developed formazans were added in 100 µl of DMSO. Finally, the absorbance was recorded at 570 nm utilizing micro-plate reader.[28, 29]

Declarations

NOTES

The authors declare no competing financial interest.

ACKNOWLEDGMENTS

The authors thank director Dr. P. Mohana Sundram PG Extension Center, Periyar University, Tamilnadu, India

References

(1) Chandran, S. P., Chaudhary, M., Pasricha, R., Ahmad, A. & Sastry, M. Synthesis of Gold Nanotriangles and Silver Nanoparticles Using Aloe vera Plant Extract. Biotechnol. Prog. 2006, 22, 577–583.
(2) Albrecht, M. A., Evans, C. W. & Raston, C. L. Green chemistry and the health implications of nanoparticles. Green Chem. 2006, 8, 417.
(3) Rouhi, J., Mahmud, S., Naderi, N., Ooi, C. R. & Mahmood, M. R. Physical properties of fish gelatin-based bio-nanocomposite films incorporated with ZnO nanorods. Nanoscale Res. Lett. 2013, 8, 364.
(4) Tiwari, V. et al. Mechanism of Anti-bacterial Activity of Zinc Oxide Nanoparticle Against Carbapenem-Resistant Acinetobacter baumannii. Front. Microbiol. 2018, 9.
(5) Kolekar, T. V. Bandgar, S. S. Shirguppikar, S. S. and Ganachari, V. S. Synthesis and characterization of ZnO nanoparticles for efficient gas sensors. Arch. Appl. Sci. Res. 2013, 5, 20–28.
(6) Narayanan, K. B. & Sakthivel, N. Green synthesis of biogenic metal nanoparticles by terrestrial and aquatic phototrophic and heterotrophic eukaryotes and biocompatible agents. Adv. Colloid Interface Sci. 2011, 169, 59–79.
(7) Sain, M. & Sharma, V. International Journal of Pure & Applied Bioscience Catharanthus roseus (An anti-cancerous drug yielding plant) - A Review of Potential Therapeutic Properties. Int. J. Pure Appl. Biosci. 2013, 1, 139–142.

(8) Asheesh, K.C. Singhal, R.A. Sharma, R.A. Govind, K. Vyas, V. Analysis of antioxidant activity of Catharanthus roseus (L.) and its association with habitat temperature. Asian J Exp Biol Sci. 2012, 3, 703–13.
(9) Nagaraj, G. et al. Facile synthesis of improved anatase TiO2 nanoparticles for enhanced solar-light driven photocatalyst. SN Appl. Sci. 2020, 2, 734.
(10) Mithun Singh Rajput, Veena Nair, Akansha Chauhan, H. J. & V. D. Evaluation of Antidiarrheal Activity of Aerial Parts of Vinca major in Experimental Animals. Middle-East J. Sci. Res. 2011, 7, 784–788.
(11) Jithendra, P., Rajam, A. M., Kalaivani, T., Mandal, A. B. & Rose, C. Preparation and Characterization of Aloe Vera Blended Collagen-Chitosan Composite Scaffold for Tissue Engineering Applications. ACS Appl. Mater. Interfaces. 2013, 5, 7291–7298.
(12) Nejatzadeh-Barandozi, F. & Enferadi, S. FT-IR study of the polysaccharides isolated from the skin juice, gel juice, and flower of Aloe vera tissues affected by fertilizer treatment. Org. Med. Chem. Lett. 2012, 2, 33.
(13) Nagaraj, G., Kowsalya, V., Chandraleka, C., Tamilarasu, S., Green Synthesis of Zn doped Catharanthus Roseus nanoparticles for Enhanced Anti-diabetic activity, RSC-Materials Advances, 2020, 1(9), 3460-3465.
(14) Ahmed, D. S. & Mohammed, M. K. A. Studying the bactericidal ability and biocompatibility of gold and gold oxide nanoparticles decorating on multi-wall carbon nanotubes. Chem. Pap. 2020, 74, 4033–4046.
(15) Nagaraj, G., Senthil, R. A., Ravichandran, K, Firmness and band gap engineered anatase TiO2 nanoparticles for enhanced visible light photocatalytic activity. IOP – Materials Research Express, 2019, 6, 095049.
(16) Saibuatong, O. & Phisalaphong, M. Novo aloe vera–bacterial cellulose composite film from biosynthesis. Carbohydr. Polym. 2010, 79, 455–460.
(17) Nagaraj, G., Dhayal Raj, A., Albert Irudayaraj, A, Next Generation of Pure Titania nanoparticles for Enhanced Solar- Light Photocatalytic Activity. Springer: Materials Science: Materials in Electronics. 2018, 29, 4373- 4381
(18) Pillay, P. P., Nair, C. P. M. & Santi Kumari, T. N. Lochnera rosea as a potential source of hypotensive and other remedies. Bull. Res. Inst. Univ. Kerala. 1959, 1, 51–54.
(19) Netala, V. R. et al. Biogenic silver nanoparticles: efficient and effective antifungal agents. Appl. Nanosci. 2016, 6, 475–484.
(20) Jaidev, L. R. & Narasimha, G. Fungal mediated biosynthesis of silver nanoparticles, characterization and antimicrobial activity. Colloids Surfaces B Biointerfaces. 2010, 81, 430–433.
(21) Kadam, A., Jangam, S., & Oswal, R. Application of green chemistry principle in synthesis of phenytoin and its biogical evaluation as anticonvulsant agents. E-Journal of Chemistry, 2011, 8(S1), S47-S52.
(22) Syeda, A. M, Riazunnisa, K. Data on GC-MS analysis, in vitro anti-oxidantand anti-microbial activity of the Catharanthus roseus and Moringa oleifera leaf extracts, Data in brief, 2020, 29, 1052582.
(23) Kabesh, K., Senthilkumar, P., Ragunathan, R., Raj Kumar, R, Phytochemical Analysis of Catharanthus roseus Plant Extract and its Antimicrobial Activity, Int. J. Pure App. Biosci. 2015, 3 (2), 162-172.
(24) Hussein, H. A., Mohamad, H., Ghazaly, M. M., Laith, A. A., & Abdullah, M. A. Cytotoxic effects of Tetraselmis suecica chloroform extracts with silver nanoparticle co-application on MCF-7, 4 T1, and Vero

cell lines. Journal of Applied Phycology, 2019, 1-17..
(25) Gabas, I. M., Stepien, G., Moros, M., Mitchell, S. G., & Jesús, M. In vitro cell cytotoxicity profile and morphological response to polyoxometalate-stabilised gold nanoparticles. New Journal of Chemistry, 2016, 40(2), 1039-1047.
(26) Atasever-Arslan, B., Yilancioglu, K., Kalkan, Z., Timucin, A. C., Gür, H., Isik, F. B., Cetiner, S. Screening of new antileukemic agents from essential oils of algae extracts and computational modeling of their interactions with intracellular signaling nodes. European Journal of Pharmaceutical Sciences, 2016, 83, 120-131.
(27) Meena, G. S., Singh, A. K., Gupta, V. K., Borad, S., Arora, S., & Tomar, S. K. Effect of pH adjustment, homogenization and diafiltration on physicochemical, reconstitution, functional and rheological properties of medium protein milk protein concentrates (MPC70). Journal of food science and technology, 2018, 55(4), 1376-1386.
(28) Mosmann, T. Rapid colorimetric assay for cellular growth and survival: application to proliferation and cytotoxicity assays. Journal of Immunological Methods, 1983, 65, 55-63.
(29) Monks, A., Scudiero, D., Skehan, P., Shoemaker, R., Paull, K., Vistica, D., Hose, C., Langley, J., Cronise, P., Vaigro-Wolff, A., Gray-Goodrich, M., Campbell, H., Mayo, J., Boyd, Feasibility of high flux anticancer drug screen using a diverse panel of cultured human tumour cell lines. Journal of the National Cancer Institute, 1991, 83, 757-766.

Figures

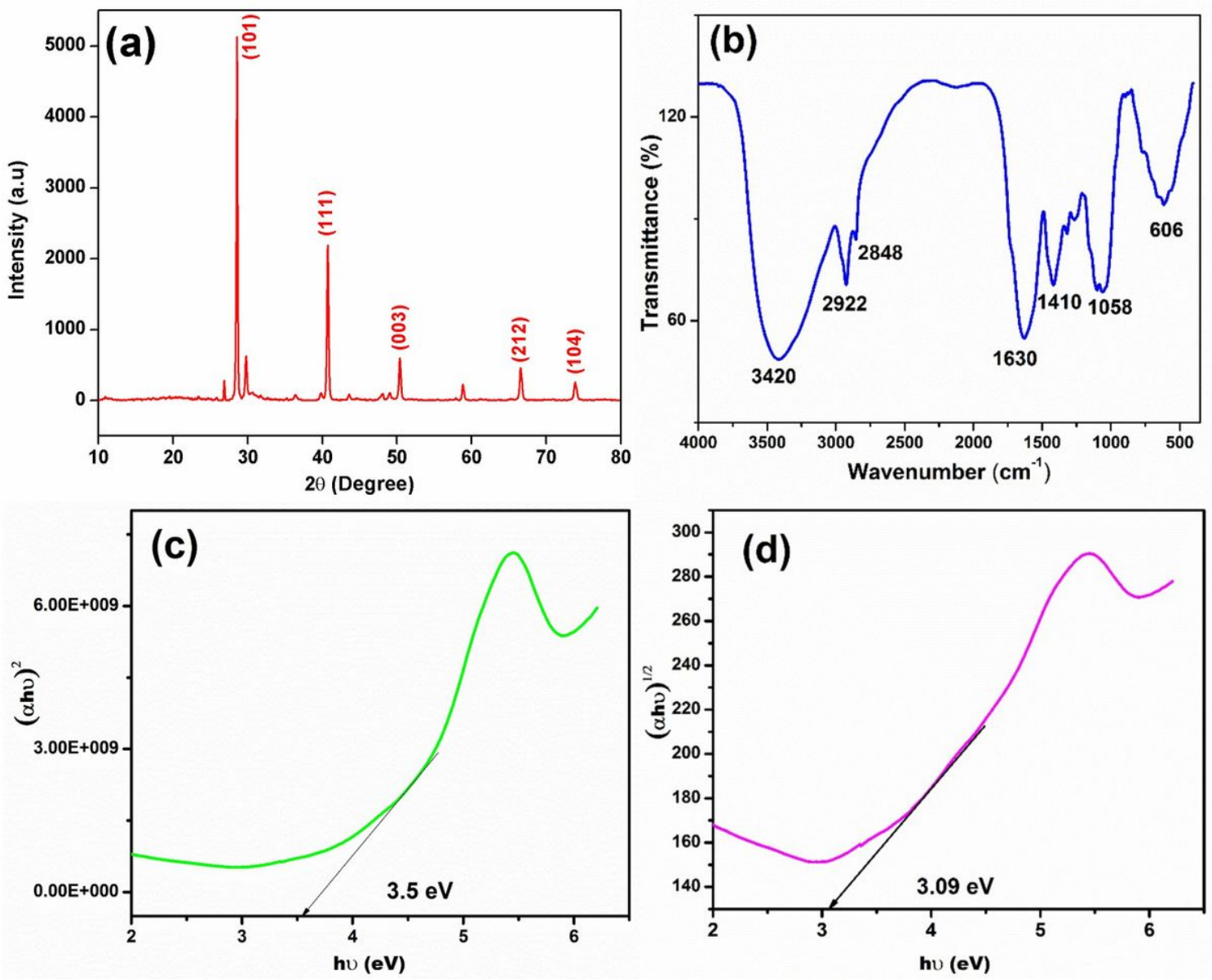

Figure 1

(a) XRD spectrum of CR NPs (b) FTIR spectrum of CR-NPs (c) UV-DRS modified Tauc plot of direct bandgap of CR-NPs (d) Indirect bandgap of CR-NPs

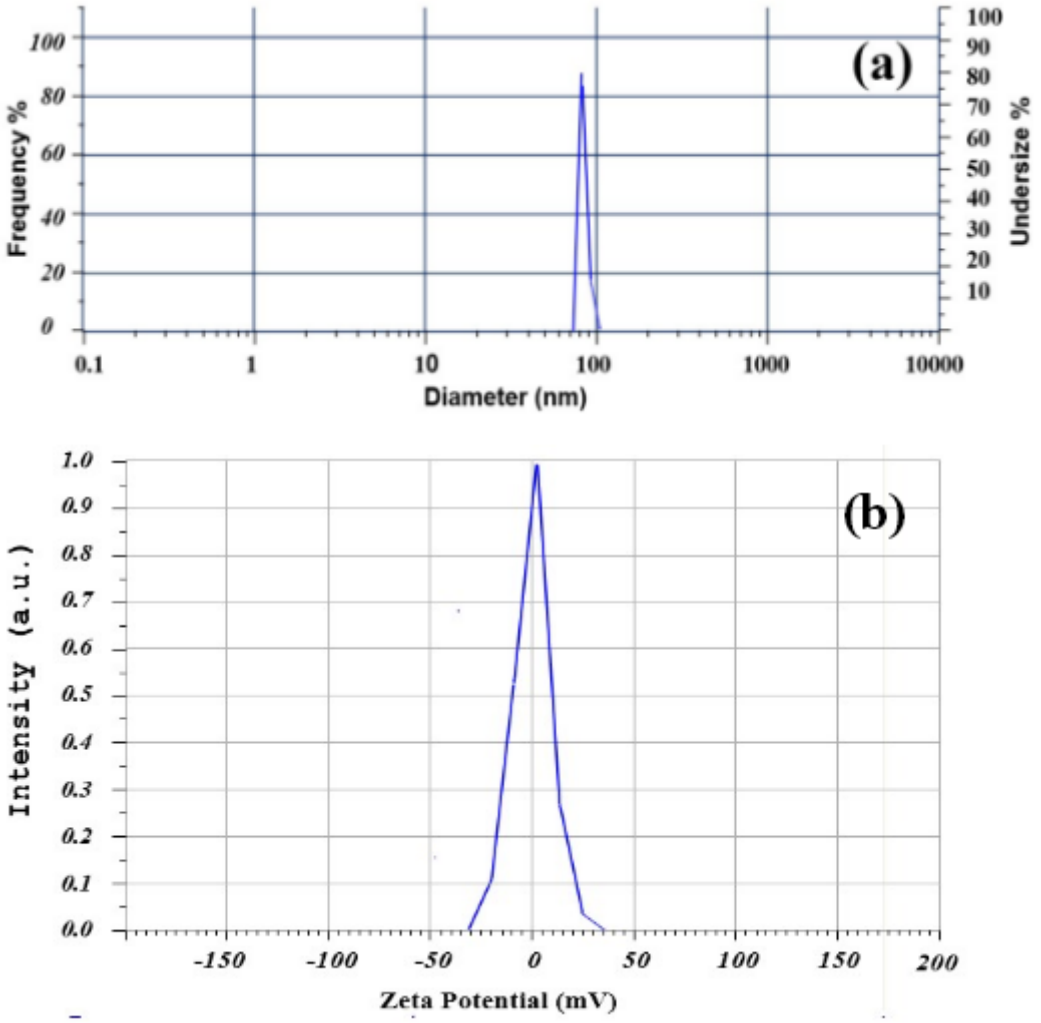

Figure 2

DLS (a) Particle size and (b) Zeta Potential of CR-NPs

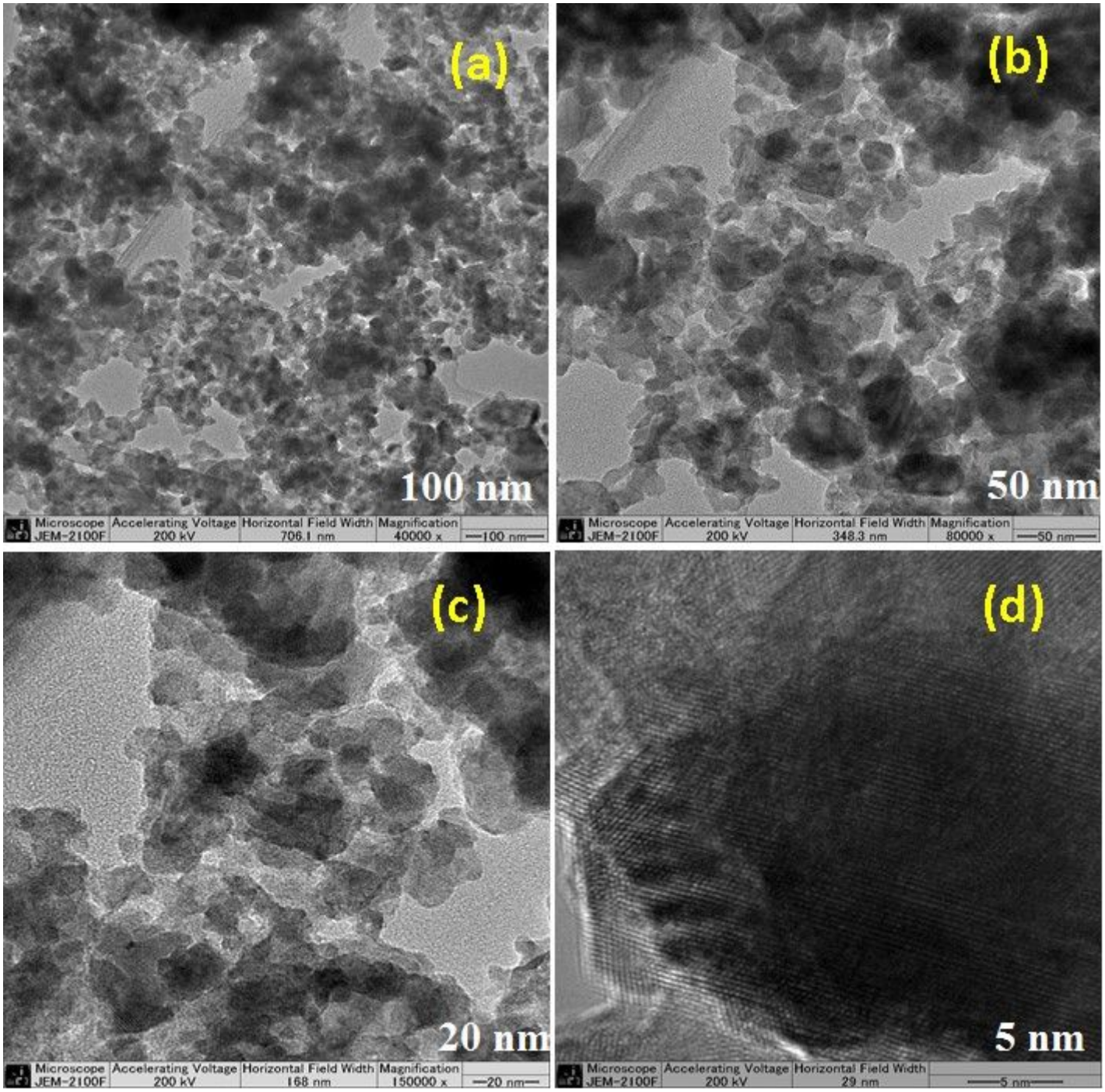

Figure 3

TEM (a, b, c) lower and higher magnification (d) lattice fringes of CR-NPs

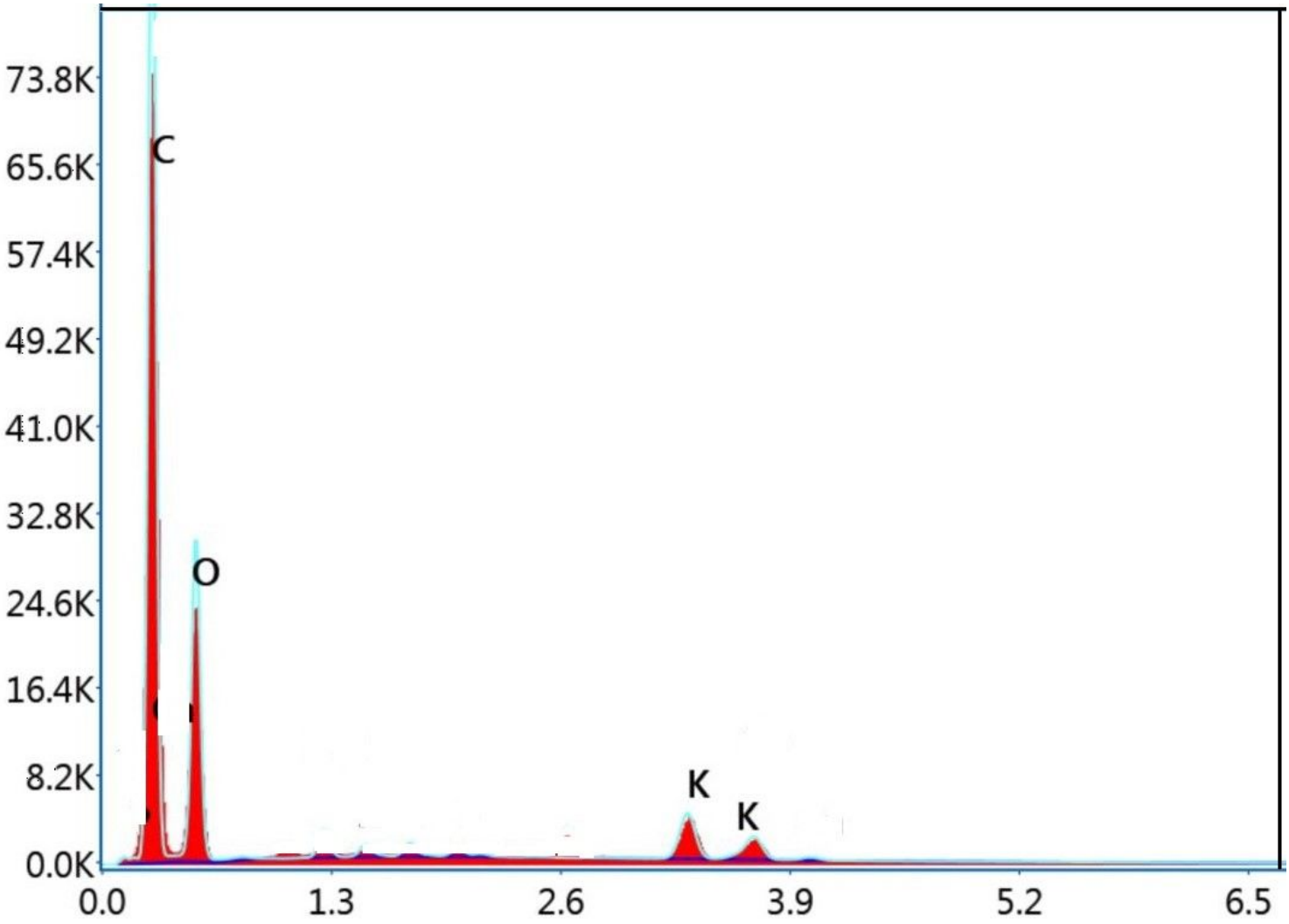

Figure 4

EDS Spectrum of CR-NPs

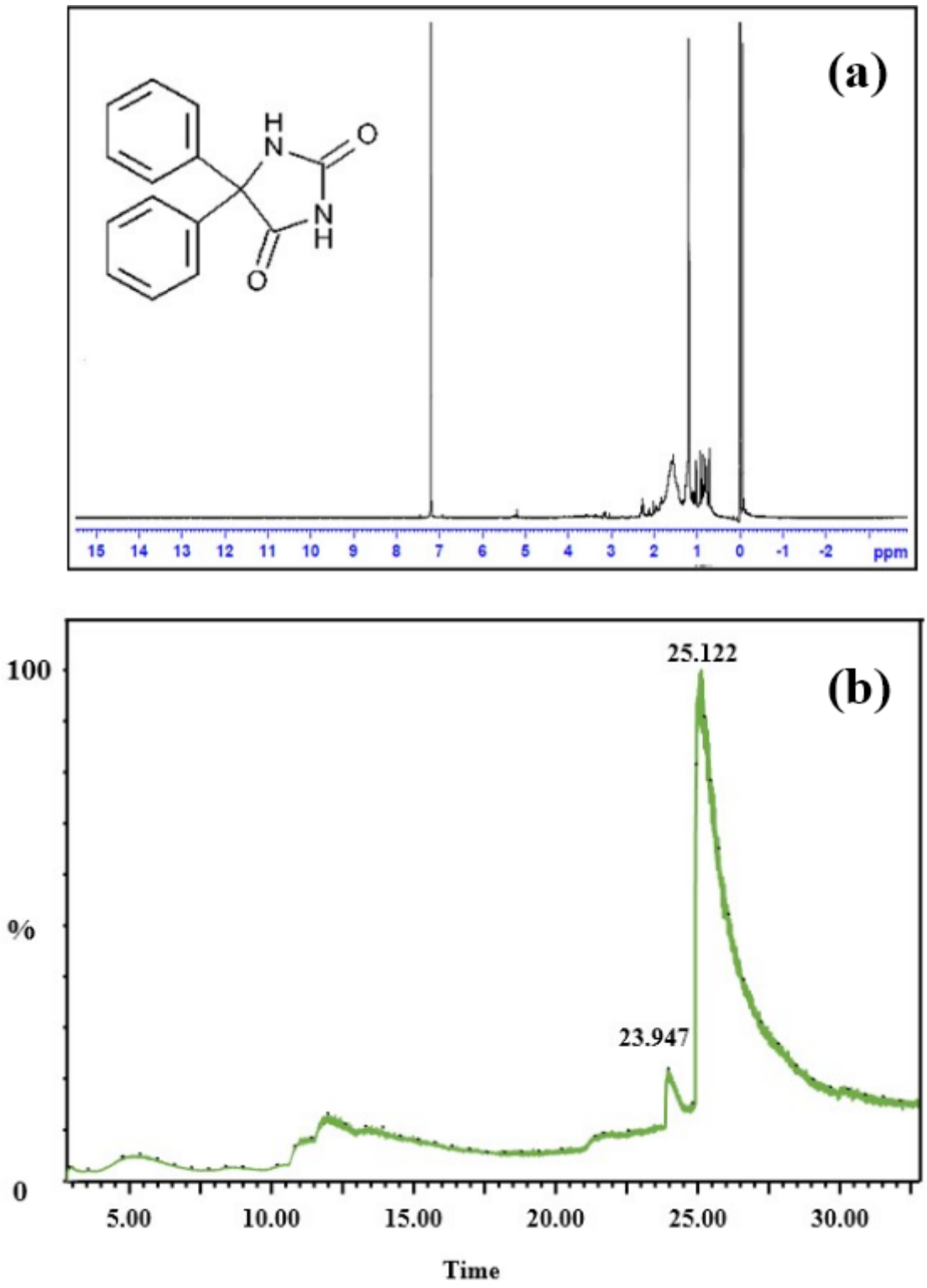

Figure 5

(a) 1H NMR chemical shift and (b) GC-MS analysis of CR-NPs

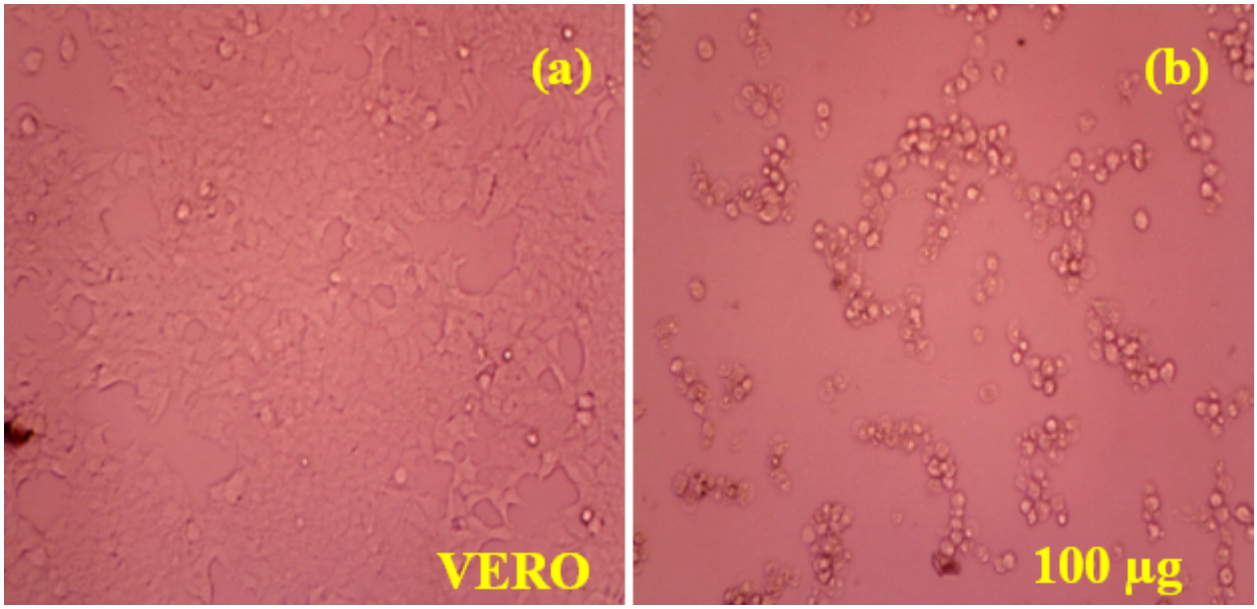

Figure 6

(a) Normal cell (VERO) and (b) CR-NPs 100 µg concentration on normal cell.

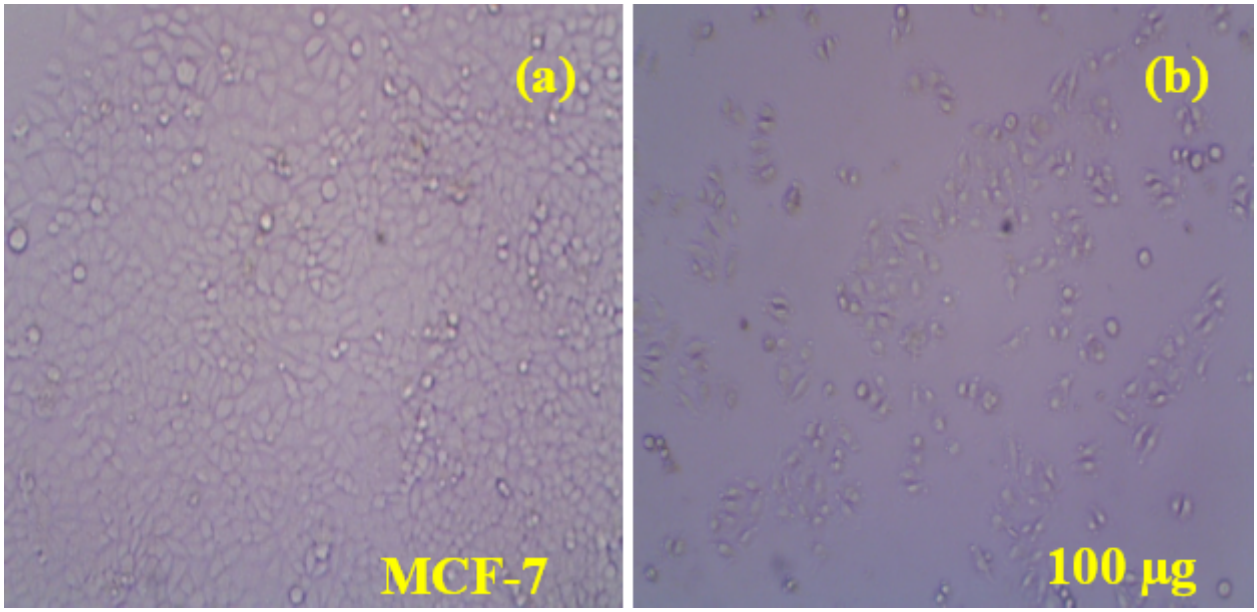

Figure 7

(a) Control sample (MCF-7) and (b) CR-NPs 100 µg concentration on MCF-7.

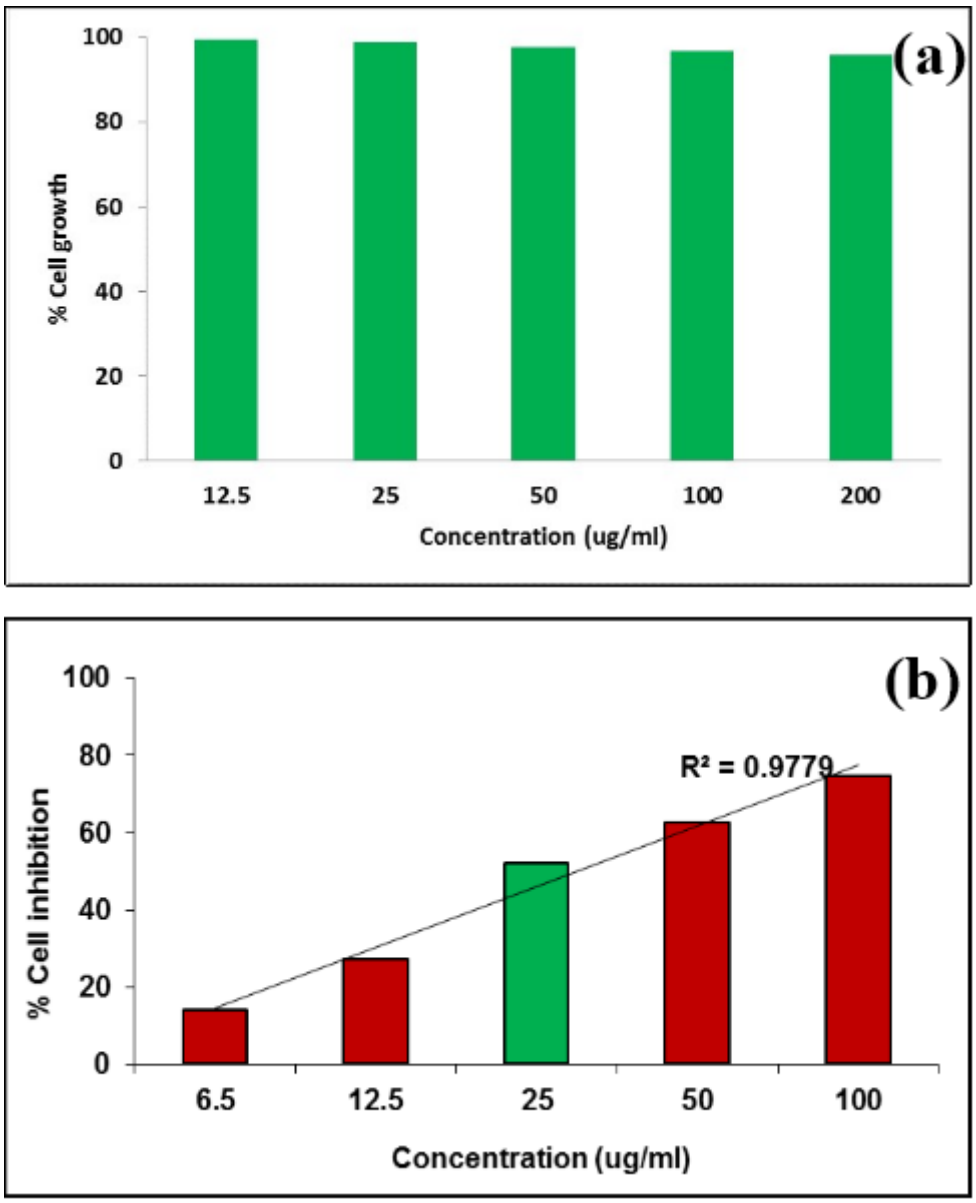

Figure 8

CR-NPs with different concentrations on (a) Vero cell line and (b) MCF-7 cell line.

Supplementary Files

This is a list of supplementary files associated with this preprint. Click to download.

- GraphicalAbstract.png